

Characteristic length scales from entanglement dynamics in electric-field-driven tight-binding chains

Devendra Singh Bhakuni^{1,*} and Auditya Sharma^{1,†}

¹*Department of Physics, Indian Institute of Science Education and Research, Bhopal, India*

We study entanglement dynamics in the nearest-neighbour fermionic chain that is subjected to both DC and AC electric fields. The dynamics gives the well known Bloch oscillations in the DC field case provided that the system size is larger than the Bloch length whereas in the AC field case the entropy is bounded and oscillates with the driving frequency at the points of dynamic localization, and has a logarithmic growth at other points. A combined AC + DC field yields super Bloch oscillations for the system size larger than the super Bloch length which puts a constraint on the device size in a typical non-equilibrium set-up to observe super Bloch oscillations where the device is connected to the leads. Entanglement entropy provides useful signatures for all of these phenomena, and an alternate way to capture the various length scales involved.

I. INTRODUCTION

A charged particle under the influence of a static electric field would be expected to undergo accelerated motion towards infinity. However, in the presence of a periodic lattice potential and electric field the motion of a quantum particle is oscillatory. These oscillations are known as Bloch oscillations [1–4]. The time period of these oscillations is inversely proportional to the field strength. Although theoretically well-understood, Bloch oscillations are hard to control experimentally in normal crystals where lattice imperfections often wash out this effect altogether [5]. However, the advent of semiconductor super-lattices, optical lattices, and temperature-tuned wave guides has made it possible to realize Bloch oscillations experimentally [6–10].

The study of Bloch oscillations in a tight-binding framework gives the well known Wannier-Stark ladder as the energies and Wannier-Stark states as the eigenstates of the Hamiltonian [11]. These states are extended over a length called *Bloch length*. Hence, to observe Bloch oscillations, the system size must be greater than this length [12]. Also, the equispaced energy spectrum results in recurrence of any initial state. Thus an initially localized state will again be localized after a Bloch period.

By making the electric field time dependent: $\mathcal{F}(t) = A \cos \omega t$, with time period $T = 2\pi/\omega$, one would expect that the same periodicity can be seen in the dynamics. However contrary to this expectation, only at certain special ratios of the amplitude and the frequency of the drive the periodicity can be seen. This phenomenon is called *dynamic localization* [13–15] and the special ratios are the roots of Bessel function of order zero.

A more general form of the electric field, which includes both AC and DC field gives other interesting effects such as *coherent destruction of Wannier-Stark localization* [16, 17], which occurs when the DC field is

resonantly tuned with the AC drive, and *super Bloch oscillations* [18–20] which occurs for slight detuning from the resonant drive. The time period of these oscillations is very large in comparison to Bloch oscillations. Similar to the static field case, a *super Bloch length* [21, 22] is associated with the super Bloch oscillations and in order to observe these oscillations the system size must be greater than this length.

Entanglement [23–25] quantifies the quantum correlations in a state between two parts of a system. In recent times, it has emerged as a unique tool to capture a vast variety of phenomena ranging from quantum phase transitions [26–28], localization/de-localization transitions [29–33], trivial to topological transition [34–36] etc. in closed systems to the correlations between a quantum dot and the baths in open quantum systems [37, 38].

The entanglement in a Wannier-Stark ladder [39] and various types of quench dynamics has been studied before, both numerically [40, 41], and using CFT calculations [42]. However, the connection to various phenomena associated with electric field was not made explicitly. From the time evolution of an initially half filled state where all the particles are filled in the left half of the chain, we find the appearance of Bloch oscillations and super Bloch oscillations in the entropy dynamics when the system size is larger than the respective length scales: Bloch length and super Bloch length. Hence, a device length greater than the super Bloch length is required if one has to observe super Bloch oscillations in a non-equilibrium set-up where the device is connected to metallic leads fixed at different chemical potentials and temperatures. Also, oscillatory behaviour of the entropy is observed at the dynamically localized point whereas a logarithmic growth in entropy is seen for the situations where a resonant drive destroys the Wannier-Stark localization.

To the best of our knowledge, the extraction of the various length scales that arise in the dynamics of a tight-binding chain subjected to electric field, from a study of entanglement is being reported for the first time in this paper. Furthermore, well-known associated phenomena like Bloch oscillations, dynamic localization, coherent de-

* devendra123@iiserb.ac.in

† auditya@iiserb.ac.in

struction of Wannier-Stark localization and super-Bloch oscillations are viewed from an entanglement perspective. The organization of this paper is as follows. In the next section, we describe the model Hamiltonian with a general time-dependent field. The subsections present the different forms of the field and the associated phenomena. The following section provides the quench protocol and the entanglement dynamics with numerical results. The summary and conclusions are given in the last section.

II. MODEL HAMILTONIAN

The Hamiltonian for a 1D tight binding model, for a finite system of size $2L$ sites with electric field is

$$H = -J \sum_{n=-L+1}^{L-1} c_n^\dagger c_{n+1} + c_{n+1}^\dagger c_n + a\mathcal{F}(t) \sum_{n=-L+1}^L (n-1/2)c_n^\dagger c_n, \quad (1)$$

where $\mathcal{F}(t)$ is the electric field and a is the lattice parameter. The numerical work is done in units where $\hbar = 1, c = 1, e = 1, J = 1, a = 1$ (unless otherwise stated). For a constant electric field $\mathcal{F}(t) = F$, the dynamics gives the well known Bloch oscillations, while a sinusoidal driving $\mathcal{F}(t) = A \cos \omega t$ can give rise to dynamic localization when A and ω are tuned appropriately. In the presence of a combined AC+DC field $\mathcal{F}(t) = F + A \cos \omega t$, the phenomenon of coherent destruction of Wannier-Stark localization is seen at resonance whereas a slight detuning from the resonant condition yields super Bloch oscillations.

A. Bloch Oscillations

For $\mathcal{F}(t) = F$, the exact eigenstates in the $n \rightarrow \infty$ limit are the Wannier-Stark states:

$$|\Psi_m\rangle = \sum_m \mathcal{J}_{n-m}(2J/aF) |n\rangle. \quad (2)$$

The single particle energies form a ladder with equal spacing $E_m = maF$, where $m = 0, \pm 1, \pm 2, \dots$. However, for finite system sizes one observes non-linear behaviour at the ends of the spectrum - these end effects are diminished on increasing system size.

A natural length scale of the problem is the Bloch length [11]

$$L_B = \frac{4J}{F}. \quad (3)$$

One can observe Bloch oscillations with the frequency $\omega_B = aF/\hbar$ in the dynamics if the system size is greater than the Bloch length. This can be easily seen by studying the time evolution of the mean square single particle width

$$\sigma^2(t) = \langle n^2(t) \rangle - \langle n(t) \rangle^2, \quad (4)$$

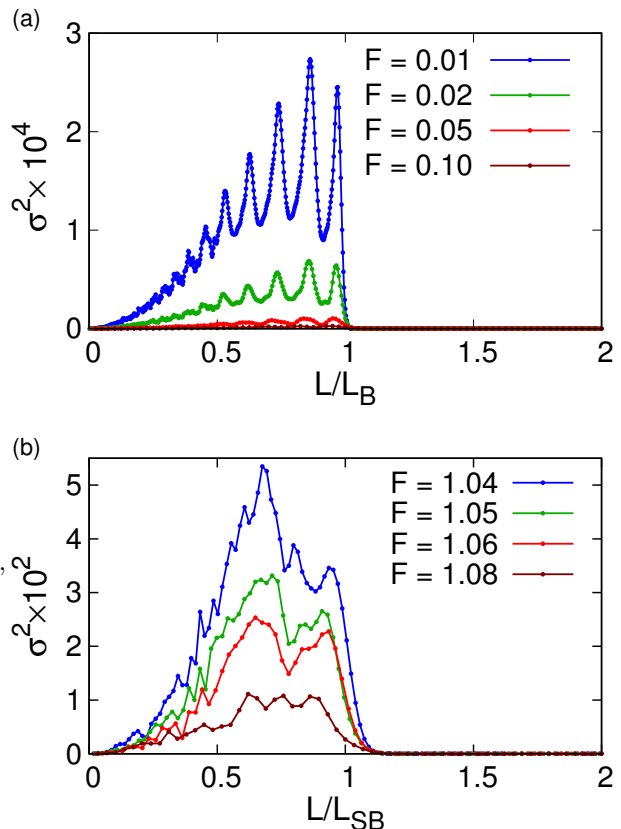


FIG. 1. Mean square single particle width of the wave-packet at $t = 5T_B$ (top) and $t = 2T_{SB}$ (bottom) as a function of system size rescaled to Bloch length and super Bloch length respectively. The transition shows the requirement of a device size greater than Bloch length and super Bloch length to observe the oscillations. (Parameters are: $A = 2.0$ and $\omega = 1.0$.)

when the initial state is a single particle localized at the centre of the chain. Time evolution for a time equal to an integer multiple of T_B must return the system back to where it started, if Bloch oscillations are present. Fig. 1(a) shows the mean square width of the wave-packet calculated for different field strengths at a time which is an integer multiple of T_B (we show data for the specific case of $5T_B$), as a function of the system size rescaled by the Bloch length. Since the initial state is a localized state with $\sigma^2 = 0$ and the same state will reappear after a Bloch period (see appendix), the mean square width at $t = nT_B$ should also go to zero. However, this happens only when the system size is larger than the Bloch length.

B. Dynamic Localization

For a time dependent electric field, the solution of the time dependent Schrödinger equation for the Hamiltonian H is given by the Houston states or accelerated

Bloch states [14, 43] as

$$|\psi_k(t)\rangle = \exp\left(-\frac{i}{\hbar} \int_0^t E(q_k(\tau)) d\tau\right) \sum_n |n\rangle \exp(inq_k(t)a), \quad (5)$$

where the quasi-momentum's time dependence can be obtained from the equation of motion as

$$q_k(t) = k + \frac{1}{\hbar} \int_0^t d\tau \mathcal{F}(\tau). \quad (6)$$

The dispersion $E(q_k) \equiv -2J \cos(q_k a)$ is that of the nearest-neighbour tight-binding model, but with implicit time-dependence from the quasi-momentum. For a sinusoidal driving $\mathcal{F}(t) = A \cos(\omega t)$, the quasi-momentum is

$$q_k(t) = k + \frac{A}{\hbar\omega} \sin(\omega t). \quad (7)$$

Although the quasi momentum $q_k(t)$ is periodic in time with period $T = 2\pi/\omega$, the Houston states however are *not* T -periodic due to an extra contribution coming from the integral appearing in the exponential. The one cycle average of that contribution is

$$\begin{aligned} \epsilon(k) &= \frac{1}{T} \int_0^T d\tau E(q_k(t)) \\ &= \frac{-2J}{T} \int_0^T d\tau \cos\left(ka + \frac{Aa}{\hbar\omega} \sin(\omega t)\right) \\ &= -2J \mathcal{J}_0\left(\frac{Aa}{\hbar\omega}\right) \cos(ka) \\ &= -2J_{\text{eff}} \cos(ka). \end{aligned} \quad (8)$$

The effect of the drive is thus the well-known renormalization of the hopping parameter. The Houston states can now be decomposed in Floquet notation with the quasi-energies $\epsilon(k)$ as

$$|\psi_k(t)\rangle = |u_k(t)\rangle \exp\left(-\frac{i}{\hbar} \epsilon(k)t\right), \quad (9)$$

where $|u_k(t)\rangle$ is T -periodic function which is obtained by removing the extra contribution term of the exponential.

Hence, the time evolution of any initial state is given by a periodic function $u_k(t)$ and the phase factors $\exp(-i\epsilon(k)t/\hbar)$. However, the phase can be tuned to unity by choosing $(\frac{Aa}{\hbar\omega})$ to be a zero of the Bessel function of order zero thereby collapsing the band. In such a scenario, the initial state will reappear after time T and a localized wave-packet remains localized. This phenomenon is known as dynamic localization.

C. Coherent Destruction of Wannier-Stark Localization and Super Bloch Oscillations

Although a static electric field destroys band formation and leads to Wannier-Stark localization and an AC driving gives dynamic localization, a combination of these

two can give rise to the counter-intuitive phenomenon of coherent destruction of Wannier-Stark localization. At resonant tuning, the effective model is the nearest-neighbor tight-binding model, and an initially localized wavepacket delocalizes according to the usual mechanism. When a slight detuning from resonance is imposed, super Bloch oscillations whose frequency is determined by the detuning are seen.

The formalism is the same as given in the previous section, however the net force is now $\mathcal{F}(t) = F + A \cos(\omega t)$. The quasi momentum given by

$$q_k(t) = k + Ft + \frac{A}{\hbar\omega} \sin(\omega t) \quad (10)$$

is *not* T -periodic except at resonance:

$$Fa = n\omega, \quad (11)$$

where n is an integer.

$$\begin{aligned} q_k(t+T) &= k + \frac{2n\pi}{aT}t + \frac{2n\pi}{a} + \frac{A}{\hbar\omega} \sin(\omega t) \\ &= k + \frac{2n\pi}{aT}t + \frac{A}{\hbar\omega} \sin(\omega t) \\ &= q_k(t), \end{aligned} \quad (12)$$

where, the periodicity of the lattice vector is used in the last step. The quasi-energies can be calculated as

$$\begin{aligned} \epsilon(k) &= \frac{1}{T} \int_0^T d\tau E(q_k(t)) \\ &= \frac{-2J}{T} \int_0^T d\tau \cos\left(ka + n\omega t + \frac{Aa}{\hbar\omega} \sin(\omega t)\right) \\ &= (-1)^n \mathcal{J}_n\left(\frac{Aa}{\hbar\omega}\right) (-2J \cos(ka)) \\ &= -2J_{\text{eff}} \cos(ka). \end{aligned} \quad (13)$$

It can be seen that AC driving leads to the formation of bands with the hopping parameter getting renormalized. Hence under such a resonant driving the particle can delocalize even though the static electric field is present. However, once again at the zeros of the Bessel function of order n , there is dynamic localization.

A slight detuning from the resonant drive gives rise to super Bloch oscillations. The off-drive condition can be written as

$$Fa = (n + \delta)\omega. \quad (14)$$

Under this condition an initially localized wave-packet starts oscillating with the time period $T_{\text{SB}} = \frac{2\pi}{\delta\omega}$ [18, 44]. These oscillations are known as super Bloch oscillations. Similar to the Bloch length, a super Bloch length is associated with super Bloch oscillations

$$L_{\text{SB}} = \frac{J \mathcal{J}_n\left(\frac{Aa}{\hbar\omega}\right)}{\delta\omega}. \quad (15)$$

The super Bloch oscillations can be seen if the system size is greater than this length. The same is shown in

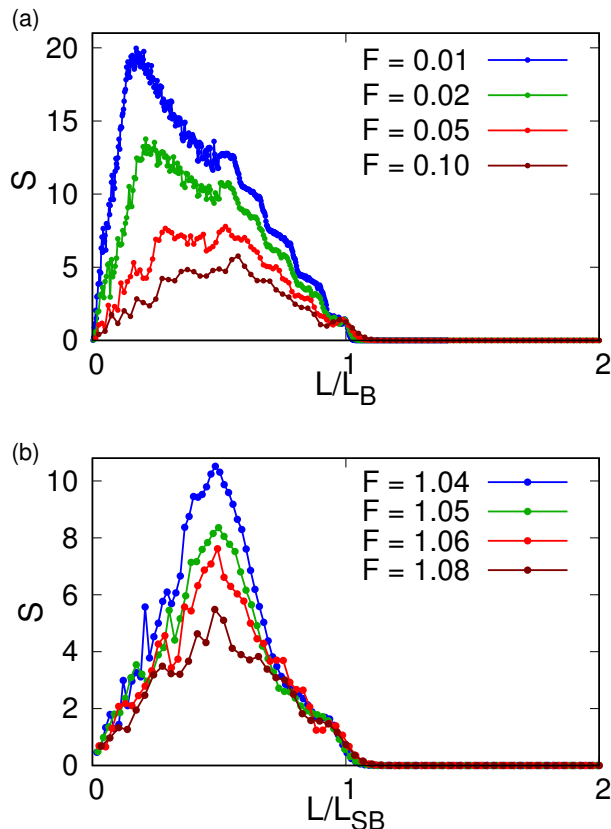


FIG. 2. Entanglement entropy as a function of L/L_B and L/L_{SB} for a DC field (top) and combined AC+DC field with slight detuning (bottom) at $t = 5T_B$ and $t = 3T_{SB}$ ($A = 2.0$ and $\omega = 1.0$). The initial state is a half-filled state where all the particles are filled on the left half of the chain. The entropy becomes zero when the system size is larger than the Bloch length and super Bloch length, respectively.

Fig. 1(b) where the wave-packet mean square width is calculated as a function of L/L_{SB} .

To summarize this section, we have made a review of the phenomena of Bloch oscillations, dynamic localization, coherent destruction of Wannier-Stark localization, and super Bloch oscillations. We have shown how the length scales L_B and L_{SB} can be extracted from a study of wave-packet width. This section sets the scene for how these phenomena may be viewed from an entanglement perspective in the next section.

III. ENTANGLEMENT ENTROPY AND QUENCH DYNAMICS

Quantum entanglement quantifies the lack of information of any subsystem despite full knowledge of the overall system, and is also a measure of how one part of the system is correlated with another part. Although various measures of entanglement are available in the literature [37, 45–47], the one that is most widely used as an

entanglement measure is the von Neumann entropy.

Let ρ be the density matrix which describes the full state of the system. The von Neumann entropy of the any subsystem A is defined as

$$S_A = -\text{Tr}(\rho_A \log \rho_A), \quad (16)$$

where ρ_A is the reduced density matrix of subsystem A , i.e. $\rho_A = \text{Tr}_B(\rho)$ with Tr_B denoting the partial trace with respect to subsystem B . When the overall state ρ is pure, the von Neumann entropy S_A is also the entanglement entropy between A and B .

In a non-interacting quadratic fermionic system, the von Neumann entropy can be directly computed from the two point correlation matrix [48] of the subsystem A : $C_{mn} = \langle c_m^\dagger c_n \rangle$. The von Neumann entropy is given in terms of the eigenvalues n_α of the subsystem correlation matrix as

$$S = \sum_\alpha [-(1 - n_\alpha) \ln(1 - n_\alpha) - n_\alpha \ln n_\alpha]. \quad (17)$$

A generalization of the above result facilitates the study of the dynamics of entanglement. The system is initially prepared in the ground state of an unperturbed Hamiltonian and then suddenly a suitable quenching Hamiltonian is switched on, and the resulting time-evolution governed by the new Hamiltonian is tracked. The time dependent correlation matrix is then directly constructed from the time evolution of the state. Finally, from the time-dependent eigenvalues of the subsystem correlation matrix, we have access to the dynamics of entanglement entropy.

The time evolution of the initial state is given by

$$|\psi(t)\rangle = e^{-iHt/\hbar} |\psi(0)\rangle \quad (18)$$

The time dependent correlation matrix can be written as

$$C_{mn}(t) = \langle \psi(t) | c_m^\dagger c_n | \psi(t) \rangle = \langle \psi_0 | c_m^\dagger(t) c_n(t) | \psi_0 \rangle, \quad (19)$$

where we have switched to the Heisenberg picture. Using the time evolution of fermionic operators c_j^\dagger and c_j , we can simplify the expression for correlation matrix as (see appendix)

$$C(t) = U^\dagger(t) C(0) U(t), \quad (20)$$

where $U_{jk}(t) = \sum_n D_{jn}^* \exp(-i\epsilon_n t/\hbar) D_{nk}$ and the matrix D diagonalizes the new Hamiltonian.

In a quenching protocol, where the final Hamiltonian includes a static electric field, the form of the unitary matrix U can be written as [11]

$$U_{nn'}(t) = \mathcal{J}_{n-n'} \left(\frac{4J}{\hbar\omega_B} \sin \frac{\omega_B t}{2} \right) e^{i(n-n')(\pi - \omega_B t)/2 - in'\omega_B t}, \quad (21)$$

Since, $U(t)$ is periodic in time with the Bloch period, the correlation matrix also follows the same periodicity. Now, the correlation matrix can be written as

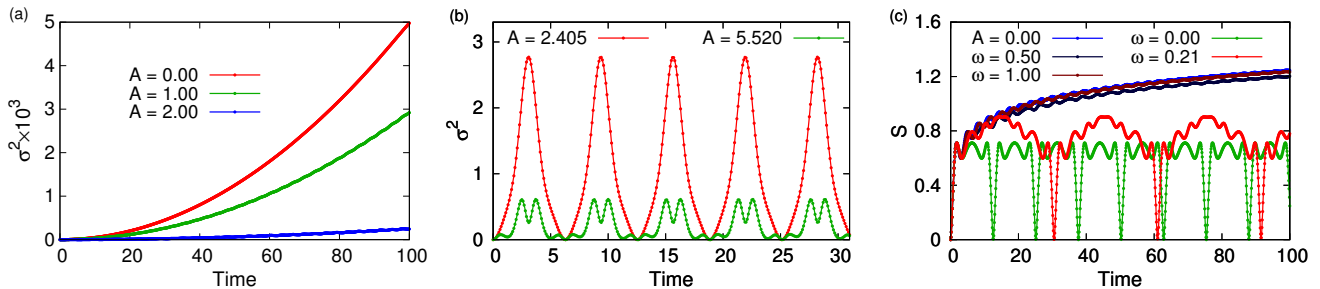


FIG. 3. Mean square width of an initially localized wave packet for an AC driving. Mean square width is unbounded for arbitrary A/ω (left), whereas it is bounded and periodic when A/ω is a root of the Bessel function of zeroth order (centre) (parameters are $L = 100$ and $\omega = 1.0$). Entanglement entropy (right) for half filled localized state. For $\omega = 0.0$, the entropy shows Bloch oscillations, whereas for other values the entropy is bounded/unbounded depending on the ratio of A/ω . (Parameters are $L = 100$, $J = 0.5$, and $A = 0.5$ for all curves except the blue one.)

$$C_{mn} = \sum_{qq'} \mathcal{J}_{q-m} \left(\frac{4J}{\hbar\omega_B} \sin \frac{\omega_B t}{2} \right) e^{-i(q-m)(\pi - \omega_B t)/2 + im\omega_B t} C_{qq'}(0) \mathcal{J}_{q'-n} \left(\frac{4J}{\hbar\omega_B} \sin \frac{\omega_B t}{2} \right) e^{-i(q'-n)(\pi - \omega_B t)/2 - in\omega_B t},$$

which in conjunction with Eqn. 17 yields the time-dependent entanglement entropy. For a time dependent Hamiltonian, we discretize the time interval into tiny regions where the Hamiltonian does not change appreciably, and the same procedure as above follows within the tiny intervals. In this case, the time evolution operator consists of a series of unitary operators.

The entanglement entropy between the two subsystems for the Wannier-Stark problem was studied in [39]. The contribution to the entanglement entropy comes from the interface width which is created by the potential gradient. Also the dynamics after turning off the electric field was studied and a logarithmic growth of the entropy was observed. However, here we entirely focus on the dynamics of the entanglement entropy after the electric field is turned *on*. The entropy as a function of system size rescaled by the Bloch length and super Bloch length at $t = 5T_B$ and $t = 3T_{SB}$ respectively, are plotted in Fig. 2. The initial state can be thought of as the ground state of a half filled nearest neighbour tight binding chain with a large electric field, where all the particles are localized to the left of the chain. A transition signifies the minimum system size to observe Bloch oscillations and super Bloch oscillations. The requirement of device length larger than the Bloch length has been given in recent work [12] where the device is connected to two metallic leads in a non-equilibrium setting and a transition from DC regime to Bloch oscillations regime is observed on varying the device size. Our finding is that a similar result holds for the super Bloch oscillations in the presence of a combined AC and DC field where the device size has to be greater than the super Bloch length.

For the case of AC driving, Fig. 3(a,b) shows that the mean square single-particle width of the wave-packet is

unbounded in time at arbitrary ratios of A/ω . In contrast, it remains bounded and oscillatory at the special ratios which are the roots of the Bessel function of order zero. The time evolution of entropy is shown in Fig. 3(c) for various parameters. One can see the Bloch oscillations in the dynamics of entropy for $\omega = 0.0$ and dynamic localization for the ratio $A/\omega = 2.405$, which is a root of Bessel function of order zero. For all other cases the entropy is unbounded in time, thus signifying de-localization. The coherent destruction of Wannier-Stark localization is shown in Fig. 4(a) for a combined AC and resonantly tuned AC field. The entropy keeps on increasing for a resonantly tuned AC, even in the presence of the DC field. However again the periodicity of the drive can be seen in the entropy at the special ratios which are now the roots of the Bessel function of order n (Fig. 4b). Super Bloch oscillations are observed in the entropy dynamics for the cases of a slight detuning from the resonant condition (Fig. 4c). The chief findings of this section are that entanglement entropy offers a useful alternative perspective for each of the phenomena associated with the application of a general (static or dynamic) electric field.

IV. SUMMARY AND CONCLUSIONS

To summarize, we studied the dynamics of many body entanglement in a nearest neighbour tight binding chain with different forms of electric field. For the static electric field we find that the dynamics captures the well known Bloch oscillations with the constraint that the system size must be greater than the Bloch length. A system size scaling of the entanglement entropy at $t = nT_B$

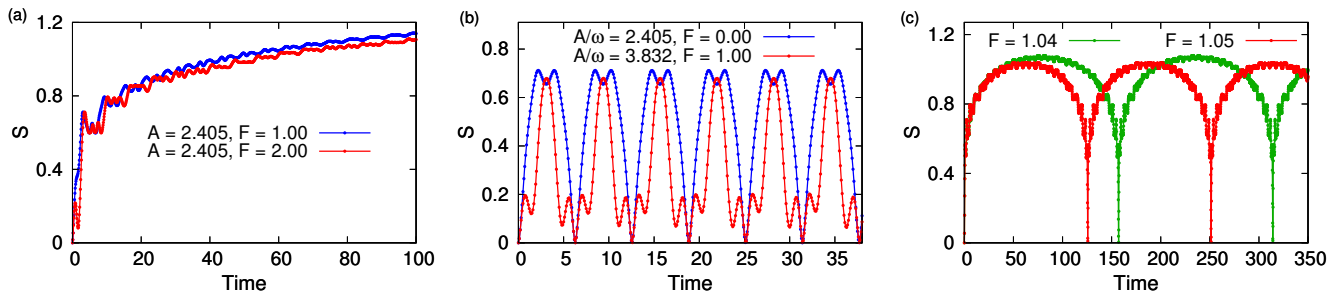


FIG. 4. Destruction of Wannier-Stark localization (left) for resonantly tuned driving $F = n\omega$, $n = 1, 2..$ and dynamic localization (centre) under the action of both static electric field and AC driving from the dynamics of entanglement entropy. Super Bloch oscillations captured by entanglement entropy for a detuning from the resonant driving(right). The parameters are $L = 100$ for all plots $J = 0.5$ for (a), (b) and $A = 3.0$ for (c).

shows a transition from a DC regime to Bloch oscillation regime. For an AC field we find that the entropy oscillates with the driving frequency at the dynamically localized point whereas at other points it is unbounded. For a combined AC+DC form of the field we find that at resonantly tuned DC field, the unboundedness of entanglement entropy verifies the coherent destruction of the localization caused by DC field whereas a slight detuning from the resonance condition leads to super Bloch oscillations in the entropy dynamics. From the system size scaling of the super Bloch oscillations, we find a transition from DC regime to super Bloch oscillations regime which demands a minimum system size to observe super Bloch oscillations.

Our results in a closed system suggests that if one has to study super Bloch oscillations in an open system which includes a set-up where a device is coupled to the metallic leads, the device size has to be greater than the super

Bloch length to observe super Bloch oscillations. We believe that the same experimental set-up, as put forward in Ref. 12 can be generalized for this purpose. Furthermore, time-dependent phenomena in a nonequilibrium set-up have mostly been studied with a small number of degrees of freedom (like a quantum dot for example). Therefore, it would be interesting to build on our current work and extend it to study non-equilibrium properties of the nearest-neighbour chain that is subjected to a time-dependent electric field.

ACKNOWLEDGMENTS

We thank Vikram Tripathi for useful discussions. A.S is grateful to SERB for the startup grant (File Number: YSS/2015/001696). D.S.B. acknowledges University Grants Commission (UGC), India for his Ph.D. fellowship.

-
- [1] C. Zener, Proceedings of the Royal Society of London. Series A, Containing Papers of a Mathematical and Physical Character **145**, 523 (1934).
- [2] G. H. Wannier, Physical Review **117**, 432 (1960).
- [3] J. Krieger and G. Iafate, Physical Review B **33**, 5494 (1986).
- [4] A. Bouchard and M. Luban, Physical Review B **52**, 5105 (1995).
- [5] P. Hofmann, *Solid state physics: an introduction* (John Wiley & Sons, 2015).
- [6] E. E. Mendez and G. Bastard, Physics Today **46**, 34 (1993).
- [7] C. Waschke, H. Roskos, K. Leo, H. Kurz, and K. Kohler, Semiconductor Science and Technology **9**, 416 (1994).
- [8] T. Dekorsy, P. Leisching, C. Waschke, K. Kohler, K. Leo, H. Roskos, and H. Kurz, Semiconductor science and technology **9**, 1959 (1994).
- [9] M. B. Dahan, E. Peik, J. Reichel, Y. Castin, and C. Salomon, Physical Review Letters **76**, 4508 (1996).
- [10] O. Morsch, J. Müller, M. Cristiani, D. Ciampini, and E. Arimondo, Physical Review Letters **87**, 140402 (2001).
- [11] T. Hartmann, F. Keck, H. Korsch, and S. Mossmann, New Journal of Physics **6**, 2 (2004).
- [12] B. S. Popescu and A. Croy, Physical Review B **95**, 235433 (2017).
- [13] D. Dunlap and V. Kenkre, Physical Review B **34**, 3625 (1986).
- [14] S. Arlinghaus, M. Langemeyer, and M. Holthaus, arXiv preprint arXiv:1103.4293 (2011).
- [15] A. Eckardt, M. Holthaus, H. Lignier, A. Zenesini, D. Ciampini, O. Morsch, and E. Arimondo, Physical Review A **79**, 013611 (2009).
- [16] M. Holthaus, G. Ristow, and D. Hone, EPL (Europhysics Letters) **32**, 241 (1995).
- [17] M. Holthaus, G. H. Ristow, and D. W. Hone, Physical review letters **75**, 3914 (1995).
- [18] K. Kudo and T. Monteiro, Physical Review A **83**, 053627 (2011).
- [19] A. R. Kolovsky, Journal of Siberian Federal University. Mathematics & Physics **3**, 311 (2010).
- [20] R. Caetano and M. Lyra, Physics Letters A **375**, 2770 (2011).

- [21] W. Hu, L. Jin, and Z. Song, *Quantum Information Processing* **12**, 3569 (2013).
- [22] E. Haller, R. Hart, M. J. Mark, J. G. Danzl, L. Reichsöllner, and H.-C. Nägerl, *Physical review letters* **104**, 200403 (2010).
- [23] N. Laflorencie, *Physics Reports* **646**, 1 (2016).
- [24] L. Amico, R. Fazio, A. Osterloh, and V. Vedral, *Reviews of modern physics* **80**, 517 (2008).
- [25] I. Peschel and V. Eisler, *Journal of physics a: mathematical and theoretical* **42**, 504003 (2009).
- [26] T. J. Osborne and M. A. Nielsen, *Physical Review A* **66**, 032110 (2002).
- [27] A. Osterloh, L. Amico, G. Falci, and R. Fazio, *Nature* **416**, 608 (2002).
- [28] G. Vidal, J. I. Latorre, E. Rico, and A. Kitaev, *Physical review letters* **90**, 227902 (2003).
- [29] N. Roy and A. Sharma, *Physical Review B* **97**, 125116 (2018).
- [30] G. Roósz, U. Divakaran, H. Rieger, and F. Iglói, *Physical Review B* **90**, 184202 (2014).
- [31] S. Bera, H. Schomerus, F. Heidrich-Meisner, and J. H. Bardarson, *Phys. Rev. Lett.* **115**, 046603 (2015).
- [32] M. Serbyn, Z. Papić, and D. A. Abanin, *Phys. Rev. Lett.* **110**, 260601 (2013).
- [33] J. H. Bardarson, F. Pollmann, and J. E. Moore, *Phys. Rev. Lett.* **109**, 017202 (2012).
- [34] R. Nehra, D. S. Bhakuni, S. Gangadharaiah, and A. Sharma, *arXiv preprint arXiv:1803.00569* (2018).
- [35] J. Sirker, M. Maiti, N. Konstantinidis, and N. Sedlmayr, *Journal of Statistical Mechanics: Theory and Experiment* **2014**, P10032 (2014).
- [36] J. Cho and K. W. Kim, *Scientific reports* **7**, 2745 (2017).
- [37] A. Sharma and E. Rabani, *Physical Review B* **91**, 085121 (2015).
- [38] H. S. Sable, D. S. Bhakuni, and A. Sharma, in *Journal of Physics: Conference Series*, Vol. 964 (IOP Publishing, 2018) p. 012007.
- [39] V. Eisler, F. Iglói, and I. Peschel, *Journal of Statistical Mechanics: Theory and Experiment* **2009**, P02011 (2009).
- [40] V. Eisler and I. Peschel, *Annalen der Physik* **17**, 410 (2008).
- [41] V. Eisler and I. Peschel, *Journal of Statistical Mechanics: Theory and Experiment* **2007**, P06005 (2007).
- [42] P. Calabrese and J. Cardy, *Journal of Statistical Mechanics: Theory and Experiment* **2007**, P10004 (2007).
- [43] W. Houston, *Physical Review* **57**, 184 (1940).
- [44] S. Longhi and G. Della Valle, *Phys. Rev. B* **86**, 075143 (2012).
- [45] J. Eisert, M. Cramer, and M. B. Plenio, *Reviews of Modern Physics* **82**, 277 (2010).
- [46] G. Vidal and R. F. Werner, *Physical Review A* **65**, 032314 (2002).
- [47] W. K. Wootters, *Physical Review Letters* **80**, 2245 (1998).
- [48] I. Peschel, *Journal of Statistical Mechanics: Theory and Experiment* **2004**, P06004 (2004).

Appendix A: Time evolution of any general quantum State

Let the initial thermal state at inverse temperature β corresponding to Hamiltonian H_0 be

$$\rho(0) = \frac{e^{-\beta H_0}}{Z}, \quad (\text{A1})$$

where, $Z = \sum_{\alpha} e^{-\beta \epsilon_{\alpha}}$. This can be express in the eigenbasis $|\Psi_n\rangle$ of the Hamiltonian H_0 as

$$\rho(0) = \frac{1}{Z} \sum_n e^{-\beta \epsilon_n} |\Psi_n\rangle \langle \Psi_n|. \quad (\text{A2})$$

At $t = 0$, a parameter of the Hamiltonian is suddenly changed. The time evolution of the initial thermal state is now govern by new Hamiltonian H_1 as

$$\rho(t) = \frac{1}{Z} \sum_n e^{-\beta \epsilon_n} |\Psi_n(t)\rangle \langle \Psi_n(t)|, \quad (\text{A3})$$

where $|\Psi_n(t)\rangle$ can be written in terms of the eigenstates of the new Hamiltonian H_1 as

$$H_1 |\Phi_n\rangle = E_n |\Phi_n\rangle \quad (\text{A4})$$

$$|\Psi_n(t)\rangle = e^{-iH_1 t/\hbar} |\Psi_n\rangle = \sum_m |\Phi_m\rangle e^{-iE_m t/\hbar} \langle \Phi_m | \Psi_n \rangle, \quad (\text{A5})$$

where E_n are the eigenvalues of H_1 . Now the time evolution of the density matrix can be written as

$$\rho(t) = \frac{1}{Z} \sum_n e^{-\beta \epsilon_n} \left(\sum_{mm'} |\Phi_m\rangle e^{-i(E_m - E_{m'})t/\hbar} \langle \Phi_{m'} | \langle \Phi_m | \Psi_n \rangle \langle \Psi_n | \Phi_{m'} \rangle \right) \quad (\text{A6})$$

In case of quenching from no electric field to some finite value of field F in the free Fermionic Hamiltonian, the eigenvalues of the final Hamiltonian are given by $E_m = maF$, where $m = 0, \pm 1, \pm 2, \dots$. Hence the time evolution of density matrix can be written as

$$\rho(t) = \frac{1}{Z} \sum_n e^{-\beta \epsilon_n} \left(\sum_{mm'} |\Phi_m\rangle e^{-ia\omega_B(m-m')t/\hbar} \langle \Phi_{m'} | \langle \Phi_m | \Psi_n \rangle \langle \Psi_n | \Phi_{m'} \rangle \right) \quad (\text{A7})$$

where, $\omega_B = aF/\hbar$ is the Bloch frequency. After a Bloch period $t = t + T_B$, we have

$$\rho(t + T_B) = \frac{1}{Z} \sum_n e^{-\beta \epsilon_n} \left(\sum_{mm'} |\Phi_m\rangle e^{-ia\omega_B(m-m')t/\hbar} e^{2\pi i(m'-m)} \langle \Phi_{m'} | \langle \Phi_m | \Psi_n \rangle \langle \Psi_n | \Phi_{m'} \rangle \right) \quad (\text{A8})$$

Since, $\exp(2\pi i(m' - m)) = 1$, we get

$$\rho(t + T_B) = \rho(t). \quad (\text{A9})$$

So, the density matrix is also periodic in time with the time period of Bloch oscillations.

Appendix B: Time evolution of a many body state and time-dependent correlation matrix

The initial Hamiltonian of the system is

$$H_0 = -\frac{1}{2} \sum_{n=-\infty}^{\infty} \left(c_n^\dagger c_{n+1} + c_{n+1}^\dagger c_n \right) \quad (\text{B1})$$

Diagonalizing the Hamiltonian H_0 , by new Fermionic operators, $b_k^\dagger = \sum_j c_j^\dagger B_{jk}$, we can take the initial state to be the ground state of H_0 as

$$|\psi(0)\rangle = \prod_{\kappa \in K} b_\kappa^\dagger |0\rangle. \quad (\text{B2})$$

After introducing the gradient term, the new Hamiltonian is given by

$$H = -\frac{1}{2} \sum_{n=-\infty}^{\infty} \left(c_n^\dagger c_{n+1} + c_{n+1}^\dagger c_n \right) + F \sum_{n=-\infty}^{\infty} \left(n - \frac{1}{2} \right) c_n^\dagger c_n \quad (\text{B3})$$

by introducing new Fermionic operators, $d_k^\dagger = \sum_j c_j^\dagger D_{jk}$, we can diagonalize the Hamiltonian H ,

$$H = \sum_k \epsilon_k d_k^\dagger d_k, \quad (\text{B4})$$

where $\epsilon_k = kaF = \hbar k \omega_B$, $k = 0, \pm 1, \dots$, and ω_B is the Bloch frequency.

The time evolution of the operator d_k^\dagger is given by

$$\frac{d}{dt} d_k^\dagger = \frac{i}{\hbar} [H, d_k^\dagger] = \frac{i}{\hbar} \epsilon_k d_k^\dagger, \quad (\text{B5})$$

which gives,

$$d_k^\dagger(t) = d_k^\dagger(0) \exp(i\epsilon_k t/\hbar). \quad (\text{B6})$$

Now the time evolution of other Fermionic operators can be written as

$$c_j^\dagger(t) = \sum_{m,n} c_n^\dagger(0) D_{nm} \exp(i\epsilon_m t/\hbar) D_{mj}^* \quad (\text{B7})$$

$$b_j^\dagger(t) = \sum_j c_n^\dagger(0) \sum_{m,n} D_{jm} \exp(i\epsilon_m t/\hbar) D_{mn}^* B_{nk}, \quad (\text{B8})$$

or,

$$b_k^\dagger(t) = \sum_j B_{jk}(t)c_j^\dagger, \quad B_{jk}(t) = \sum_{m,n} D_{jm} \exp(i\epsilon_m t) D_{mn}^* B_{nk}(0). \quad (\text{B9})$$

So the time evolution of the ground state can be written as

$$|\psi_0(t)\rangle = \prod_{\kappa \in K} b_\kappa^\dagger(t)|0\rangle \quad (\text{B10})$$

$$|\psi(t)\rangle = \prod_{\kappa \in K} \left(\sum_j c_\kappa^\dagger(0) B_{jk}(t) \right) |0\rangle \quad (\text{B11})$$

If we translate the time by a Bloch period $T_B = 2\pi/\omega_B$, the state becomes

$$|\psi(t + T_B)\rangle = \prod_{\kappa \in K} \left(\sum_j c_\kappa^\dagger(0) B_{jk}(t + T_B) \right) |0\rangle, \quad (\text{B12})$$

now,

$$B_{jk}(t + T_B) = \sum_{m,n} D_{jm} \exp(i\epsilon_m(t + T_B)/\hbar) D_{mn}^* B_{nk}(0) = \sum_{m,n} D_{jm} \exp(i\epsilon_m t/\hbar) D_{mn}^* B_{nk}(0) \exp(2\pi i m). \quad (\text{B13})$$

Since, $\exp(2\pi i m) = 1$, we have

$$B_{jk}(t + T_B) = B_{jk}(t) \quad (\text{B14})$$

Hence, the state $|\psi_0(t)\rangle$ is periodic in time with the time period equal to the Bloch period T_B .

The time dependent correlation matrix can be written as

$$C_{mn}(t) = \langle \psi(t) | c_m^\dagger c_n | \psi(t) \rangle = \langle \psi(0) | c_m^\dagger(t) c_n(t) | \psi(0) \rangle \quad (\text{B15})$$

using the time evolution of Fermionic operators c_j^\dagger and c_j we can write the expression for the time dependent correlation matrix as

$$C_{mn}(t) = \sum_{pq} \sum_{p'q'} D_{qp} \exp(i\epsilon_p t) D_{pm}^* C_{qq'}(0) D_{q'p'}^* \exp(-i\epsilon_{p'} t) D_{p'n}. \quad (\text{B16})$$

Which can be simplifies to

$$C(t) = U^\dagger(t) C(0) U(t), \quad (\text{B17})$$

where $U_{jk}(t) = \sum_n D_{jn}^* \exp(-i\epsilon_n t) D_{nk}$ and matrix D diagonalizes the final Hamiltonian.